ARMY RESEARCH LABORATORY

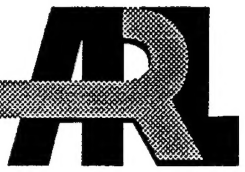

Generation of Advanced Optical Modulators Using the Piezoelectric Effect

Richard H. Wittstruck

ARL-TR-1118 August 1996

NOTICES

Disclaimers

The findings in this report are not to be construed as an official Department of the Army position, unless so designated by other authorized documents.

The citation of trade names and names of manufacturers in this report is not to be construed as official Government endorsement or approval of commercial products or services referenced herein.

REPORT DOCUMENTATION PAGE

Form Approved
OMB NO. 0704-0188

1. AGENCY USE ONLY *(Leave blank)*	2. REPORT DATE	3. REPORT TYPE AND DATES COVERED
	August 1996	Technical Report

4. TITLE AND SUBTITLE
GENERATION OF ADVANCED OPTICAL MODULATORS USING THE PIEZOELECTRIC EFFECT

5. FUNDING NUMBERS

6. AUTHOR(S)
Richard H. Wittstruck

7. PERFORMING ORGANIZATION NAMES(S) AND ADDRESS(ES)
US Army Research Laboratory (ARL)
Physical Sciences Directorate
ATTN: AMSRL-PS-DE
Fort Monmouth, NJ 07703-5601

8. PERFORMING ORGANIZATION REPORT NUMBER
ARL-TR-1118

9. SPONSORING / MONITORING AGENCY NAME(S) AND ADDRESS(ES)

10. SPONSORING / MONITORING AGENCY REPORT NUMBER

11. SUPPLEMENTARY NOTES

12a. DISTRIBUTION / AVAILABILITY STATEMENT
Approved for public release; distribution is unlimited.

12 b. DISTRIBUTION CODE

13. ABSTRACT *(Maximum 200 words)*

In recent years, interest in the realization of optical modulators has been on the rise due to several device breakthroughs which employ the quantum confined Stark effect (QCSE). This family of devices has demonstrated remarkably high contrast ratio (7000:1) and optical switching speed (10^{-12} sec) parameters. While these devices have surpassed their conventional self electro-optic effect device (SEED) counterparts in performance and utility, they lack multimode, room temperature operation due to the need for a thermally induced strain between the substrate and the epitaxial layer. One potential solution to this issue is the introduction of a piezoelectric substrate which would afford a critical degree of freedom in the magnitude and direction of induced strain required to achieve multimode room temperature operation. This report proposes an integrated parametric model which defines the required material and device design/performance characteristics for attaining the next generation of spatial light modulators. These modulators will be critical components in achieving real time, optical target recognition capability on the battlefield.

14. SUBJECT TERMS	15. NUMBER IF PAGES
Optical modulation; piezoelectric effect	25
	16. PRICE CODE

17. SECURITY CLASSIFICATION OR REPORT	18. SECURITY CLASSIFICATION OF THIS PAGE	19. SECURITY CLASSIFICATION OF ABSTRACT	20. LIMITATION OF ABSTRACT
Unclassified	Unclassified	Unclassified	UL

TABLE OF CONTENTS

LIST OF FIGURES

1.0 INTRODUCTION

Before a detailed discussion of optical modulating devices can be undertaken, an understanding of several phenomena must be achieved which explain why modulators can accomplish their prescribed operation.

The first of these effects is the Franz - Keldysh effect. Published in 1958 in two separate treatises (Ref 1), these two men described the effect an applied electric field can have on the fundamental bandedge of a semiconductor.

An illustrative way to see this proof is to consider a Zener diode (Figure 1). As the reader will recall, the diode is a p-n type comprised of degenerate doping levels (p & n > 10 exp 18 cm^{-3}) operated under reverse bias conditions. Associated with such operation is the energy band diagram of Figure 2.

A valence electron seeking an interband transition can traverse the energy spectrum (into the conduction band) in two ways:

(1) Absorb energy $h\omega > E_g$ providing it sufficient energy to elevate to the conduction band (a very unlikely scenario given the environment).

(2) Tunnel through an energy barrier to reach the conduction band.

Let us consider approach (2). The valence electron is confronted with a barrier of height, E_g, and thickness, t, through which it must tunnel (Figure 3). Obviously, a relation exists between the force produced by the applied electric field and the barrier as follows;

$$qE = E_g / t$$

thus:

$$t = E_g / qE$$

when energy (i.e., photon or phonon) absorption occurs, it can decrease the barrier height by a value, $h\omega$. Hence,

$$t = E_g - h\omega / qE$$

As can be seen from this equation, a reduction in the barrier width would be produced and would certainly increase the probability of tunneling in accordance with Yang's equ. 4-45 (Ref. 28, p. 108). In order to elucidate this point, one can begin with

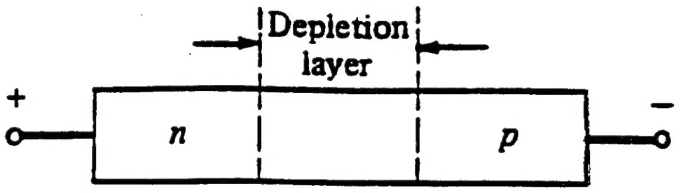

Figure 1 - Zener diode cross section

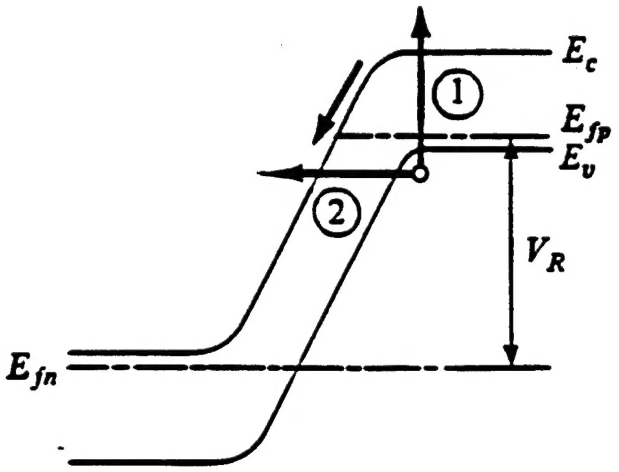

Figure 2 - Zener diode energy band diagram

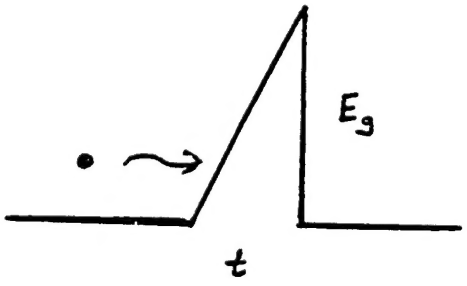

Figure 3 - Zener tunneling mechanism schematic

Yang's equation and derive the more familiar Zener tunneling equation (Ref. 27, p. 198, equ. 13-19) in terms of the bandgap energy and the electric field.

$$T_{tunneling} = \exp \frac{-8\pi\, x_d \{2q\, m_e\, \chi_b\}^{1/2}}{3h}$$

(Let: $x_d = t$ & $q\chi_b = E_g$)

$$T_{tunneling} = \exp \frac{-8\pi\, t \{2\, m_e\, E_g\}^{1/2}}{3h}$$

(Recall: $t = E_g / qE$)

$$T_{tunneling} = \exp \frac{-8\pi \{2\, m_e\}^{1/2} E_g^{3/2}}{3h\, qE}$$

(Divide top & bottom by 2π)

$$T_{tunneling} = \exp \frac{-4 \{2\, m_e\}^{1/2} E_g^{3/2}}{3\hbar\, qE}$$ Q.E.D.

In the case of absorption taking place at a level less than the bandgap energy, this equation can be rewritten as :

$$T_{tunneling} = \exp \frac{-4 \{2\, m_e\}^{1/2} (E_g - h\omega)^{3/2}}{3\hbar\, qE}$$

We can see from this equation that absorption beneath the fundamental bandedge will result in an increase of Zener tunneling probability (which is dependent on the applied electric field). The pending question is: "By what mechanism does this absorption occur?"

When considering traditional E-k relationships in a direct band semiconductor, we make several assumptions:

(1) One electron traverses throughout a periodic potential (i.e., lattice).

(2) No allowed singularity at the conduction band minimum and valence band maximum.

(3) Ignore the Coloumbic interaction between the e-h pair (created in an interband transition).

If we remove assumption (3), we find, at low thermal energy, this Coloumbic attraction binds the e-h pair producing a quasi-particle known as an exciton (Figure 4). The exciton can be viewed as the first excited state of one electron energy band possessing binding energies of:

$$E_n^{ex} = 13.6\,(1/n\varepsilon_r)^2\,(m_r / m_e) \quad eV$$

(n = integer ; m_r = reduced mass ; ε_r = dielectric constant)

As can be seen from Figure 4, the exciton is not localized but allowed to move throughout the entire crystal as a "particle" with effective mass, $M = m_e + m_h$. In k-space, the binding energies become:

$$E_n^{ex}(k) = E_n^{ex} + (\hbar^2 k^2 / 2M)$$

Shown below (without proof) is the effect these exciton absorptions have on the overall absorption coefficient;

$$\alpha_n(\hbar\omega) = 2.7 \times 10^5\,(2\,m_r / m_e)^{3/2}\,f\,(\hbar\omega - E_g - E_n^{ex})^{1/2}\,(n_r)^{-1} \quad cm^{-1}$$

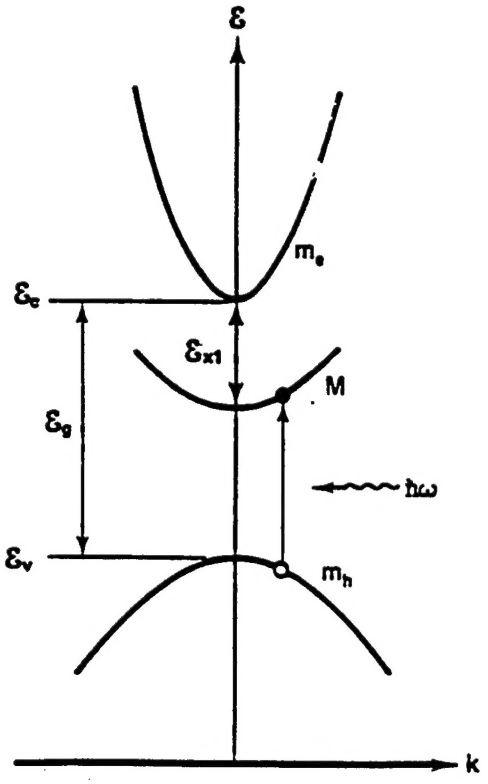

Figure 4 - Exciton creation mechanism

where: f = oscillator strength = $1 + (m_e / m_h)$

$$m_r = \frac{M + m_h}{M m_h}$$

n_r = refractive index

We can see an effect (thermal, electrical, strain, etc.) induced shift in the exciton energy would result in a change of the isotropic absorption coefficient. This energy shift (for a multiple quantum well (MQW)) can be seen as:

$$\Delta E_n^{ex} \cong -3 \times 10^{-20} (m_e + m_{hh}) E^2 d_{QW}^4 \quad eV$$

resulting in an anisotropic exciton absorption coefficient (shown for heavy hole case only):

$$\alpha_{ex}(\hbar\omega) \cong \frac{2.9 \times 10^3}{n_{QW} d_{QW} \Gamma} \exp \frac{-(E_n^{ex} - \hbar\omega)^2}{2^{1/2}\Gamma^2}$$

(Γ = exciton linewidth)

Thus, a shift in exciton energy induced by an "effect" will alter the absorption coefficient of the semiconductor. This is accomplished due to the resultant change in dielectric constant which occurs (the reader is referred to the Kramers-Kronig relation for a more in-depth explanation of this change and its role in changing the imaginary part of the refractive index). Hence, this mechanism forms the basis for modulators which take advantage of electroabsorption changes to perform their operation.

In order to maximize this electro-optic effect, one would design a structure to absorb energy (i.e., photon from an optical beam) as close to the exciton resonance peak as possible without completely overlapping it (for fear of full absorption and non-radiative recombination).

An alternate mechanism is Wannier Stark (W-S) localization. Wannier-Stark localization has been observed by two research groups (Ref 13, 18). This effect states that when an electric field is applied normal to the MQW (i.e., parallel to the growth axis), a series of localized, quantized electron eigenstates occur over a length:

$$\lambda = E_g / qE$$

(λ = wavelength of the tunneling electron)

All groups have reported no such effect observed in bulk materials. These materials tend to reflect the well known Franz-Keldysh effect only. However, the introduction of an MQW with a barrier width tailored to the wavelength of the electron seems to promote W-S localization. Empirical data suggests that at a high field limit:

$$\frac{qE\, n_{QW}\, d_{QW}}{E_g} \geq 1$$

the superlattice behaves as a series of uncoupled quantum wells as the electric field is increased beyond a critical value (See Fig 5). Another way to see this is to examine the PL data at various electric fields (See Fig. 6). One can clearly see a shift, a sharpening and a change in magnitude of the interband transition linewidth as we progress from low fields through moderate fields to high fields.

A famous relationship which has become the signature of W-S localization is the inverse proportionality between the absorption coefficient and electric field. When this phenomenon is observed, the so - called "Stark ladder" of energy states has been deduced from the data. The absorption peak (Bloch) oscillates with respect to the applied field. While it has been shown that the superlattice acts as a series of uncoupled wells at high field, it is assumed only adjacent wells undergo this phenomenon (at moderate fields) and can contribute to the overall effect.

Using W-S localization as a basis, let us consider what could happen WITHIN a single QW. If the applied field can overcome the Coloumbic attraction between e-h pairs residing in the same well, the force induced by the field can separate (confine) the electrons and holes to opposite sides of the well. This separation would lead to a lifting of the Krammers degeneracy (i.e. splitting of the light and heavy hole bands). Evidence for this effect is seen when one observes a variation in the hole (lh;hh) effective mass under field. This variation induces a change in the exciton binding energy (i.e., broadening of the transitions) for increasing electric field. The exciton effective mass is dependent upon the sum of the lh and hh masses and the electron mass.

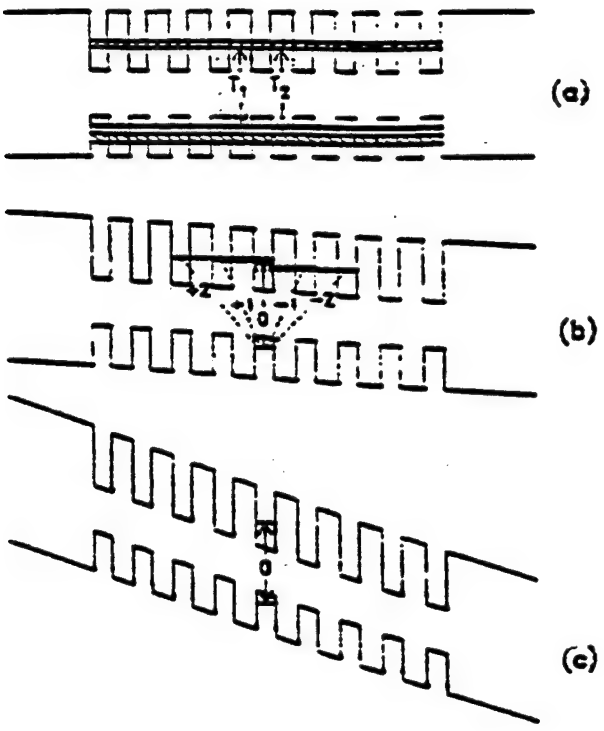

Figure 5 - Conduction- and valence-band profiles for
(a) small, (b) moderate, and (c) high electric field

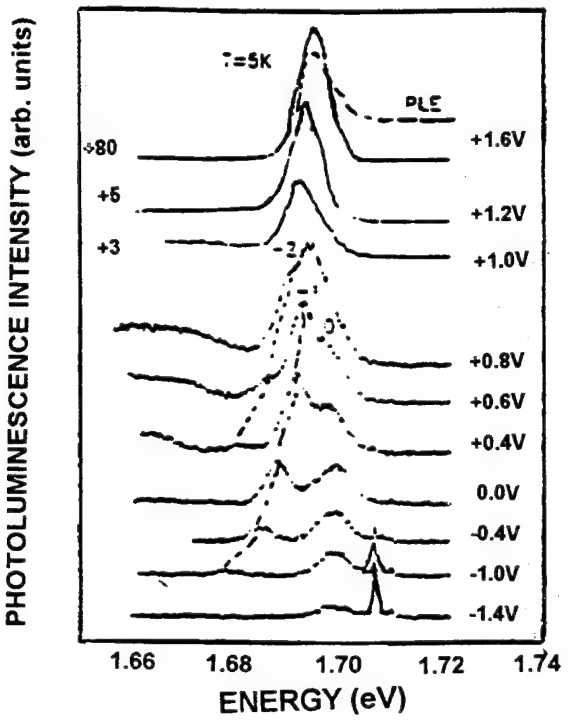

Figure 6 - Photoluminescence spectra

This overall effect is a quantum confinement of states which maximizes the separation of electron and hole wavefunctions (intrawell) and establishes a mechanism for fast switching of light incident upon the modulator via the modulation of the electroabsorption (which is dependent on the effective mass changes).

This quantum confined Stark effect (QCSE) forms the basis for the device studied in this paper.

2.0 SUBSTRATE CHARACTERISTICS - BIAS VICE STRAIN RELATIONSHIP

Historically, the induced strain in the epitaxial layer has been provided via epitaxially lifting off (ELO) a film and "bonding" it, using Van der Waal forces, to a prescribed substrate having preferential orientation cuts. Thus, via thermal annealing, the strain orientation and magnitude has been "frozen" into the epitaxial layer.

The governing equations for such a mechanism involve the lattice constant of the epitaxial layer, the substrate and the annealing/operating temperatures as follows for the x-y plane;

$$\varepsilon_{xx}(T) = \int_{T_O}^{T} [a_x(T) - a_{MQW}(T)]\, dT$$

$$\varepsilon_{yy}(T) = \int_{T_O}^{T} [a_y(T) - a_{MQW}(T)]\, dT$$

This technique is laborious and provides for a single mode device operated at low temperatures. What if we were to replace the candidate substrate with a piezoelectric material capable of providing this induced strain via the (converse) piezoelectric effect. This effect would provide a direct relationship between the applied bias (i.e., electric field) and the corresponding strain which is REVERSIBLE with a change of polarity. In addition, the ability to provide biaxial strain would be made simpler since there would now exist a simple matrix relation between constituent parts of the x-y plane. This mechanism would create a multi-mode, room temperature operating device whose mode would be strictly governed by the applied bias or frequency.

In general the matrix relationship between induced strain and applied electric field can be shown to be:

$$S_j = d_{ij} E_i$$

For the purpose of illustrating the theory, we will use the 422 crystal class. This class is uniquely interesting for it provides the simplest matrix relation for achieving induced strain. This simplicity allows the theory to reduce to a manageable set of linear equations.

Class 422 ; SHEAR Strain

Assume $Bi_{12}SiO_{20}$

Sillenite

$V := 2$ volts $\qquad t := 10^{-6}$ m

$d := 40 \cdot 10^{-12} \frac{coul}{newton} \qquad E := \frac{2}{10^{-6}} \frac{V}{m}$

$$S := \begin{pmatrix} 0 & 0 & 0 & d & 0 & 0 \\ 0 & 0 & 0 & 0 & -d & 0 \\ 0 & 0 & 0 & 0 & 0 & 0 \end{pmatrix} \cdot \begin{bmatrix} 0 \\ 0 \\ 0 \\ E \\ 0 \\ 0 \end{bmatrix}$$

$$S := \begin{pmatrix} .00008 \\ 0 \\ 0 \end{pmatrix}$$

From this simple illustration, we deduce that for a sillenite substrate of thickness 1 micron, we can apply a bias of 2 volts to produce an induced strain in the x- direction of .008%.

3.0 DEVICE DESIGN CHARACTERISTICS

Consider the structure of Figure 7. As light is passed through the spatial light modulator (SLM) structure, several parameters are affected leading to the required modulation of light. These parameters are defined below.

INTENSITY OUTPUT:

$$I(V) = I_o(V)\{\mathrm{SIN}^2[\theta(V) - \theta_{OFF}] + \mathrm{COS}[2\theta(V)]\,\mathrm{COS}[2\theta_{OFF}]\,\mathrm{SIN}^2[\Delta\phi(V)/2]$$

INTENSITY AT SLM :

$$I_o(V) = I_{INC}\, e^{-\alpha(V)\,d}$$

$$(d = d_{QW} \times \mathrm{number}_{QW})$$

ISOTROPIC ABSORPTION COEFFICIENT:

A theoretical or empirical method may be employed as follows;

Calculate: $\alpha(V) = \mathrm{Im}\{A_j (E - E_j + i\Gamma_j)^{-1} + B_j \ln[\Gamma_j + i(E - E_j - E_j^{ex})]\}$

where: { j = 1 (hh), 2 (lh) }

or

Empirical: $$E = \frac{V}{(d_{QW} + d_B) \times n_{QW}}$$

POLARIZATION ANGLE OF ROTATION:

$$\theta(V) = \arctan[\exp(\Delta\alpha d / 2)] - 45^{\circ}$$

ANISOTROPIC ABSORPTION COEFFICIENT:

$$\Delta\alpha(V) = \alpha(V)\left[\pm 2\,(3)^{1/2}\,\mathrm{SIN}(2\phi) / (2 \pm \mathrm{COS}(2\phi))\right]$$

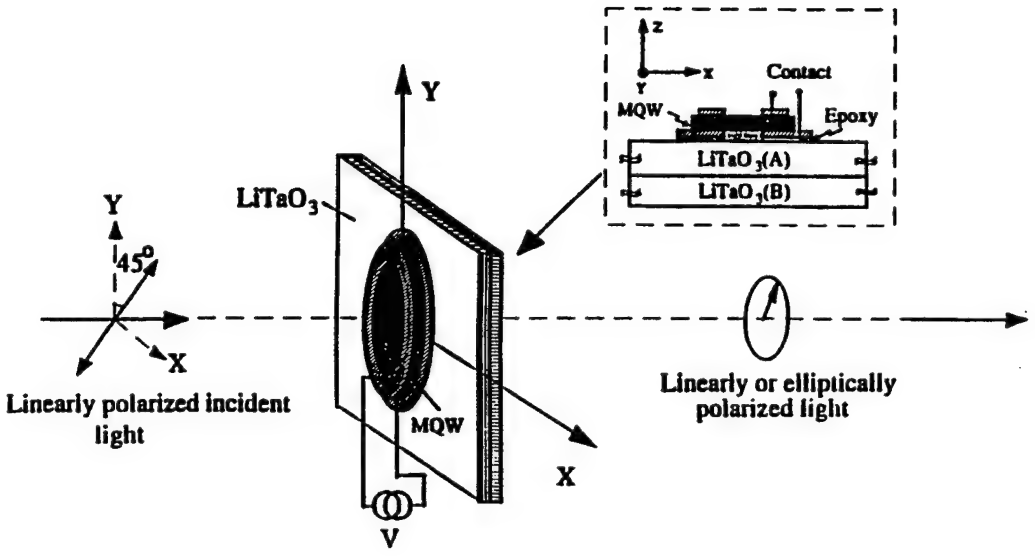

Figure 7 - Proposed device structure and testing configuration; insert: a cross section of the device

PHASE RETARDATION ANGLE:

$\phi = \text{ARCTAN}\,[\,(3)^{1/2}\,\eta\,/\,(1 + (1+3\eta^2)^{1/2})]$

where: $\eta = \dfrac{\Delta E_s}{\Delta E_{QW} + (1 - 2\gamma)\,\Delta E_s'}$

$\Delta E_s = b\,(\varepsilon_{xx} - \varepsilon_{yy})\;;\; \Delta E_s' = b\,(\varepsilon_{xx} + \varepsilon_{yy})$

$\gamma = S_{12} / S_{12} + S_{11}$

$\varepsilon_{xx}(T) = {}_{To}\!\int^{T} [a_x(T) - a_{MQW}(T)]\,dT$

$\varepsilon_{yy}(T) = {}_{To}\!\int^{T} [a_y(T) - a_{MQW}(T)]\,dT$

RELATIVE PHASE RETARDATION ANGLE:

$\Delta\phi = 2\Pi\,\Delta n / \lambda$

[Δn (BIREFRINGENCE) = $n_x - n_y$ IS MEASURED EMPIRICALLY]

n = index of refraction

4.0 PERFORMANCE CHARACTERISTICS

CONTRAST RATIO:

$\text{C.R.} = \dfrac{I(V^{ON})}{I(V^{OFF})}$

POWER DISSIPATION:

ELECTRIC POWER PROVIDED --> P = Watts / Area (S)

OPTICAL POWER AT SLM --> $I_{INC}(1 - e^{-\alpha(V)d})$

OPTICAL POWER ABSORBED AT 2ND POLARIZER:

$| I_{INC} e^{-\alpha(V)d} - I(V) |$

MODULATION DEPTH:

10 LOG (P_{TRANS} {ON}) - 10 LOG (P_{TRANS} {OFF})

5.0 EXAMPLE

In order to illustrate this model, the following numerical example is used;

ASSUMPTIONS:

V	=	14 volts	I	=	1 μA
W	=	14 μW		S =	9×10^{-4} cm^2
d_{QW}	=	80Å	d_B	=	60 Å
n_{QW}	=	150	Γ_j	=	4 meV (@ R.T.)
θ_{OFF}	=	0°	b	=	2 eV
a_x	=	16.2×10^{-6} / °C	$a_y = a_{QW}$	=	6.2×10^{-6} / °C
ε_{yy}	=	0	T_o	=	150 °C
ε_{zz}	=	$\gamma(\varepsilon_{xx} + \varepsilon_{yy}) \approx \gamma\varepsilon_{xx}$	I_{INC}	=	1 (NORMALIZED)
V_{OFF}	=	14 V	IDEAL QW (i.e., NO FLUCTUATIONS)		
V_{ON}	=	0 V	λ = 845 nm		

CALCULATED FROM STANDARD QUANTUM WELL HAMILTONIAN

E_j = 1.424 + .059 = 1.483 eV

E_j^{ex} = 8 meV (hh); 7 meV (lh)

CALCULATED FROM
LUTTINGER-KOHN HAMILTONIAN

$$H_\varepsilon = \begin{pmatrix} \tfrac{1}{2}[\Delta E_{QW} + \Delta E_S'(1 - 2\gamma)] & (3^{1/2}/2)\,\Delta E_S \\ (3^{1/2}/2)\,\Delta E_S & \tfrac{1}{2}[\Delta E_{QW} + \Delta E_S'(1 - 2\gamma)] \end{pmatrix}$$

ΔE_{QW} = 10 meV

5.1 DESIGN ISSUES

(1) I (V) = 5×10^4 (a.u. @ V_{ON})
10 (a.u. @ V_{OFF})

(2) I_o (V) = 5×10^4 (a.u. @ V_{ON})
4×10^3 (a.u. @ V_{OFF})

(3) α(V) = 20,000 cm^{-1}

(4) θ (V) = 15°

(5) $\Delta\alpha$ (hh) = 7700 cm^{-1} (V_{ON})
5400 cm^{-1} (V_{OFF})

(6) ϕ = 37°

where: γ = .12 %

(7) $\Delta\phi$ = 30°

5.2 PERFORMANCE ISSUES

(1) CONTRAST RATIO:

C.R. = 5000 : 1 (@ R.T.)

(2) ELECTRIC POWER PROVIDED --> 15.5 mW/cm^2

OPTICAL POWER AT SLM --> 1 W/cm^2

(3) OPTICAL POWER ABSORBED AT 2ND POLARIZER:

.11 W/cm^2

(4) MODULATION DEPTH: 37 dB

6.0 CONCLUSION

It can be seen by this simple treatise that the use of piezoelectrically driven strain may provide the incremental engineering performance improvement required to allow attainment of the next generation of SLM. This strain requirement is solely dependent on the choice of the correct material and the ability to grow that material as pure as possible to avoid defect - related anomalies from occurring which would degrade the SLM performance.

The realization of such devices for practical use will result in the implementation of optical pattern recognition systems, for target recognition, which provide high contrast, high speed, real time threat analysis.

BIBLIOGRAPHY

1. Z. W. Franz, Naturforsch, 13a, 484; L.V. Keldysh, Sov. Phys. - JETP 7, 788.

2. U. Efron, Spatial Light Modulator Technology Materials, Devices and Applications, Marcel Dekker, Inc. (1995).

3. M. Cardona, Modulation Spectroscopy, Academic Press (1969).

4. J.F. Nye, Physical Properties of Crystals, Oxford Science Publications (1992).

5. C. Wolfe, Physical Properties of Semiconductors, Prentice Hall (1989).

6. K.W. Jelley, et al., Applied Physics Letters, 55(1), 3 July 1989, Siemens Corporate Research, Inc.

7. J. Singh, et al., Journal of Lightwave Technology, Vol. 6, No. 6, June 1988, University of Michigan and Rockwell International Corporation.

8. M.S. Leeson, et al., IEE Proc.-Optoelectron., Vol. 141, No. 4, August 1994, Manchester Metropolitan University, U.K.

9. H.J. Bakker, et al., Phys Rev A, June 1990, FOM-Institute for Atomic and Molecular Physics, The Netherlands.

10. R. Hui, IEEE Photonics Technology Letters, Vol. 2, No. 10, October 1990, Fondazione Ugo Bordoni, Rome, Italy.

11. Y-C Chan, et al., IEEE Photonics Technology Letters, Vol. 5, No. 12, December 1993, University of Tokyo, Japan.

12. M.F. Ferreira, et al., IEE Proceedings, Vol. 137, Pt. J, No. 6, December 1990, University of Aveiro, Portugual.

13. J.M. Kuo, et al., IEEE Transactions on Electronic Devices, Vol. 36, No. 11, November 1989, AT&T Bell Labs, Murray Hill.

14. E.E. Mendez, et al., Physical Review Letters, Vol. 60, No. 23, 6 June 1988, IBM, Yorktown Heights.

15. M.S. Alam, et al., IEEE Proceedings, 1992, University of Dayton.

16. E. Bigan, et al., IEEE Transactions Photonics Technology Letters, Vol. 3, No. 12, December 1991, CNET.

17. S. Domrachev, IEEE/URSI Proceedings of the International Semiconductor Device Research Symposium, December 1993, Institute of Mechanics and Physics, Saratov State University, Russia.

18. T. Feng, et al., IEEE Journal of Quantum Electronics, Vol. 24, No. 3, March 1988, Beijing University, China.

19. P. Voisin, et al., Physical Review Letters, Vol. 61, No. 14, 3 October 1988, CNET.

20. H. Shen, et al., Applied Physics Letters, 62(23), 7 June 1993, ARL, Fort Monmouth.

21. H. Shen, et al., IEEE Photonics Technology Letters, Vol. 6, No. 6, June 1994, ARL, Fort Monmouth.

22. H. Shen, et al., 1993 IEDM Proceedings, ARL, Fort Monmouth.

23. H. Shen, et al., Physical Review B, Vol . 47, No. 20, 15 May 1993, ARL, Fort Monmouth.

24. H-C Kuo, M.S. Thesis for Rutgers ECE Department, (defended 26 April 1995).

25. H. Shen, et al., Uniaxial Strained MQW SLM, U.S. Patent 5, 274, 247, January 1994.

26. R. Wittstruck, et al., Dynamic Modulation of Quantum Devices, U.S. Patent Application, 08/388,100, 31 March 1995.

27. A. Husain, Proceedings of 1994 ARPA Optoelectronics Review, June 1994.

28. K. Hess, Advanced Theory of Semiconductor Devices, Prentice Hall, 1988.

29. E. Yang, Microelectronic Devices, McGraw Hill, 1988.

30. J. Singh, Semiconductor Optoelectronics, McGraw Hill, 1995.

31. A. Ballato, Piezoelectricity: Venerable Effects, Modern Thrusts; ARL Technical Report, 8 December 1993, ARL, Fort Monmouth

32. B. Lalevic, Asst. Notes of EE 16:330:584, March 1995.

Defense Technical Information Center*
ATTN: DTIC-OCC
8725 John J. Kingman Rd, STE 0944
Fort Belvoir, VA 22060-6218
(*Note: Two DTIC copies will be sent from STINFO office, Ft Monmouth, NJ)

Director
US Army Material Systems Analysis Actv
ATTN: DRXSY-MP
(1) Aberdeen Proving Ground, MD 21005

Commander, AMC
ATTN: AMCDE-SC
5001 Eisenhower Ave.
(1) Alexandria, VA 22333-0001

Director
Army Research Laboratory
ATTN: AMSRL-D (John W. Lyons)
2800 Powder Mill Road
(1) Adelphi, MD 20783-1197

Director
Army Research Laboratory
ATTN: AMSRL-DD (COL Thomas A. Dunn)
2800 Powder Mill Road
(1) Adelphi, MD 20783-1197

Director
Army Research Laboratory
2800 Powder Mill Road
Adelphi, MD 20783-1197
(1) AMSRL-OP-SD-TA (ARL Records Mgt)
(1) AMSRL-OP-SD-TL (ARL Tech Library)
(1) AMSRL-OP-SD-TP (ARL Tech Publ Br)

Directorate Executive
Army Research Laboratory
Physical Sciences Directorate
Fort Monmouth, NJ 07703-5601
(1) AMSRL-PS
(1) AMSRL-PS-A (V. Rosati)
(1) AMSRL-PS-T (M. Hayes)
(1) AMSRL-OP-FM-RM
(22) Originating Office

Advisory Group on Electron Devices
ATTN: Documents
Crystal Square 4
1745 Jefferson Davis Highway, Suite 500
(2) Arlington, VA 22202

Commander, CECOM
R&D Technical Library
Fort Monmouth, NJ 07703-5703
(1) AMSEL-IM-BM-I-L-R (Tech Library)
(3) AMSEL-IM-BM-I-L-R (STINFO Ofc)

Deputy for Science & Technology
Office, Asst Sec Army (R&D)
(1) Washington, DC 20310

HQDA (DAMA-ARZ-D/
Dr. F.D. Verderame)
(1) Washington, DC 20310

Director
Naval Research Laboratory
ATTN: Code 2627
(1) Washington, DC 20375-5000

USAF Rome Laboratory
Technical Library, FL2810
ATTN: Documents Library
Corridor W, STE 262, RL/SUL
26 Electronics Parkway, Bldg 106
Griffiss Air Force Base
(1) NY 13441-4514

Dir, ARL Battlefield
Environment Directorate
ATTN: AMSRL-BE
White Sands Missile Range
(1) NM 88002-5501

Dir, ARL Sensors, Signatures,
Signal & Information Processing
Directorate (S3I)
ATTN: AMSRL-SS
2800 Powder Mill Road
(1) Adelphi, MD 20783-1197

Dir, CECOM Night Vision/
Electronic Sensors Directorate
ATTN: AMSEL-RD-NV-D
(1) Fort Belvoir, VA 22060-5806

Dir, CECOM Intelligence and
Electronic Warfare Directorate
ATTN: AMSEL-RD-IEW-D
Vint Hill Farms Station
(1) Warrenton, VA 22186-5100

Cdr, Marine Corps Liaison Office
ATTN: AMSEL-LN-MC
(1) Fort Monmouth, NJ 07703-5033